Particle Motions in Fluid Interfaces and Through Perforations

Daniel D. Joseph

University of Minnesota

April 2002

The following topics are proposed for study:

I. Particle transport through perforations. The aim is to find the dimensionless parameters for which the screening of particles in viscoelastic fluids occur and to elucidate the underlying mechanics.

II. The remarkable cleaning properties of viscoelastic liquid films laden with small particles. Remediation of oil slicks.

III. Motions due to capillarity of floating particles on liquid surfaces.

1. Vertical force balance
2. Horizontal force balance
3. Dynamics

IV. Studies of transient free motions leading to self-assembly of floating particles.

V. Direct numerical simulation of motions of solid spheres in liquid-air interfaces.

VI. Method of correlations.

VII. Pattern formation arising in self-assembled aggregates of particles in fluid surfaces in forced motions.

VIII. Surface active properties of colloidal and nanoparticles embedded in liquid surfaces with applications pointing to the stabilization of emulsions and core-annular flows.

IX. Nanoparticle assembly in vitrified liquid films.

Movie animations relevant to the project proposed here can be viewed in film clips collected on our dedicated web page, http://www.aem.umn.edu/research/particles.

This [draft 2] proposal has hyperlinks to movie animations. Blue italic text calls your attention to locating the links *often as photographs with a border*. Underlined blue text also has a hyperlink, but requires an available Internet connection. The movies that came with this PDF file should reside in the same directory to enable off-line viewing of them without an Internet connection [which the first draft required].

I Particle transport through perforations

We studied the transport of slurries through holes in the device shown in figure I.1. Suction and injection experiments comparing the transport properties of Newtonian and viscoelastic fluids (1% aqueous polyox solutions) were carried out. Both types of fluids are pumped for transport of proppants for reservoir fracturing applications. Unexpected screening properties of slurries in polyox solutions were found and form one focus for the studies proposed here. For given values of the particle concentration ϕ, the ratio of particle to tube diameter and $E = \lambda\eta /_{\rho}D_p^{2}$ elasticity number, there is a critical velocity U_c above which particles are screened and do not pass through the tube. When the volume fraction of solids is large, the particles will go through. Smaller particles enter the perforation more easily. The more viscoelastic the fluid, the greater is the screening effect in which particles do not go through.

Some properties of screening of particles being sucked into the tube through tubeless siphon are exhibited in the photographs and explained in the caption to figures I.2, I.3 and I.4. The flow properties of viscoelastic and Newtonian are dramatically different, just the opposite (see figure I.5), even when there are no particles present so that something like the presence of screening in polymeric liquids and its absence in pure solvent might not be surprising. Videos of experiments showing screening in suction and injections can be viewed on our web page.

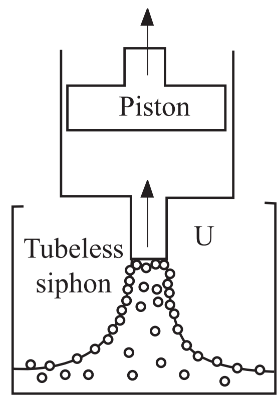

Figure I.1. Particle transport through tubes (perforations). When the piston moves up, fluid from the bottom chamber is sucked up and a tubeless siphon is formed. Injection of particles from the top chamber occurs when the piston is moved down. Under certain to-be-determined conditions, particles cannot be sucked through or blown out. This is called screening. When the superficial tube velocity $U < U_c(\phi, D_p/D_T, E)$*, particles go through; when* $U > U_c$ *they don't go through.* ϕ *is the solids,* D_p/D_T *the ratio of particle to tube diameter* $E = \lambda n/D_p^2$ *is the elasticity number where* λ *is the relaxation time,* η *the viscosity and* ρ *is density. The screening increases with* E*; in the Newtonian case* E = 0*, particles always go through.*

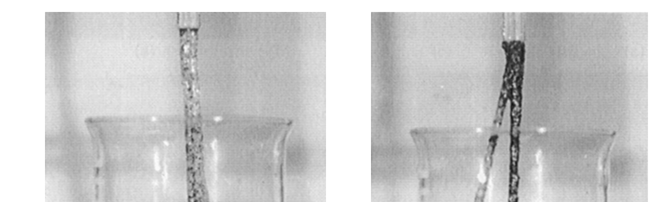

Figure I.2. (After Boonacker, 1999.) Particles rising on a tubeless siphon. The siphon arises from sucking fluid from the bottom chamber of the device shown in figure I.1, pulling up the piston. (a) The long filament of fluid is held together by extensional stresses which are supported by the polymeric liquid (1% aqueous polyox) used in this study. The tubeless siphon cannot occur in Newtonian fluids. Here we show something new, particles embedded in fluid rise in the siphon and are blocked from entering the tube until the penetration of particles at tube entrance rises above a critical value (see figure I.3 and I.4). Particles seem to preferentially select the liquid-air surface. (b) The siphon will sometimes split into two streams, one up (left), the other down (right).

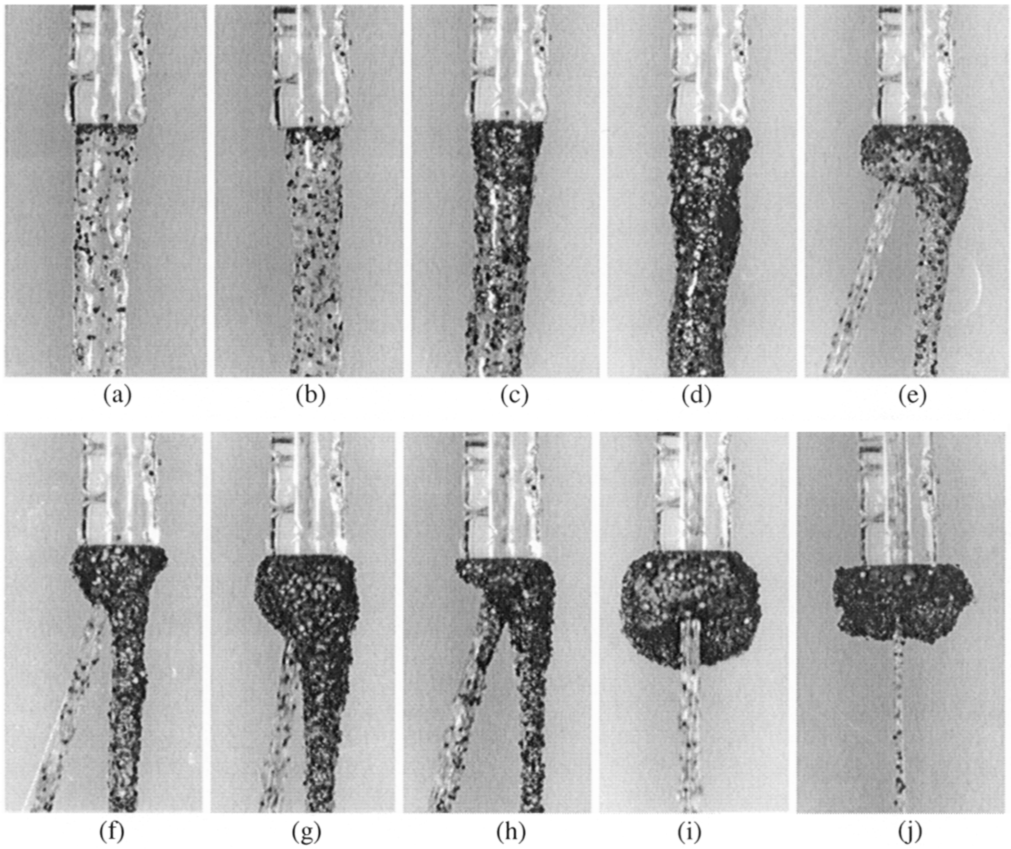

Figure I.3. (After Boonacker, 1999.) This sequence of pictures shows that a tubeless siphon screens particles at the tube entrance. In (e)–(h) the stream of fluid on the left is the up flow, while the right stream is the down flow. Some particles start to go up the tube in picture (e).

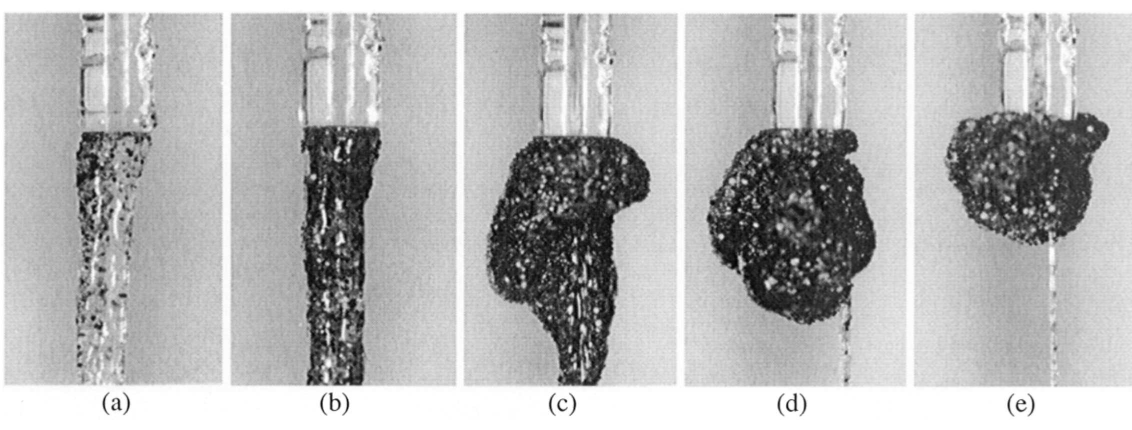

Figure I.4. (After Boonacker, 1999.) This sequence shows an alternate form of the tubeless siphon. The siphon does not always break into two streams. Here the screened particles flow downwards on the outside of the up-flowing core. Some particles start to go up the tube in picture (c).

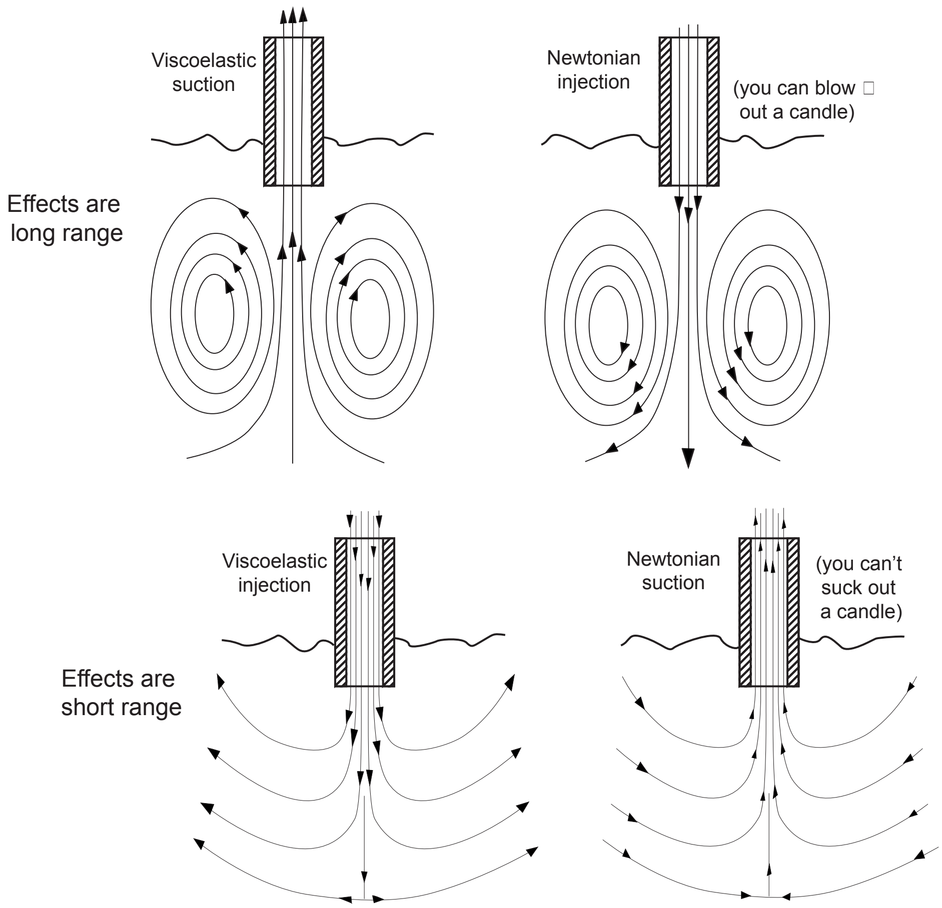

Figure I.5. Asymmetry of suction and injection in Newtonian and viscoelastic fluid (just the opposite).

The goal of this research ion screening is to predict the conditions for screening and more broadly to predict the volume flow rates of slurries through perforations. We have already established the existence of a screening function

$$f(U,\phi, D_P/D_T, E) = 0 \qquad (I.1)$$

whose borders we propose to determine from experiments. It is likely that the extrusion velocity would be better expressed as a Reynolds number whose exact form is to be determined.

Injection of particles through perforations is important in various applications. Sometimes it is desirable in various applications, sometimes it is desired to promote transport. Perforated linear and gravel packs are used to screen sand from oil from producing oil-baring sounds entering perforated pipelines and oil wells. The perforations are usually circles or slits. In the other applications, like slurry pumping, it is desired to move particles freely through perforations The controlling parameters which we propose to study,

1) Ratio of particle to perforation size.
2) The fluids (Newtonian, viscoelastic)
3) The shape of the perforations: circle, square, red
4) Shape of the Particle: natural sands vs. spheres
5) Polydispersity or size span of particles in a slurry

We plan to study these topics using the piston driven devices shown in figure I.1. Though we have not found systematic studies of this type on the topics (I-VI) proposed here for study, a number of papers concerning the gravel packs used to screen particles and the forming of sand arches screening particle transport at perforations have been studied. Coberly and Wagner (1938) suggested that a gravel pack having granular particles of diameter 10 times the formation grain size would provide effective sand control. Hill (1941) suggested that the ratio be reduced to 8, but failures were still noted. The effects of polydispersity were considered by Winterburn (1947) who states that "actual experience in the field has shown that sand entry can be virtually eliminated by the use of gravel which is approximately 10 times the grain size of the 10 percentile of the finest sand to be screened." Though finer gravel will obviously do a more effective job in screening sand it will also decrease the permeability of the gravel pack, reducing production; there is a trade-off. A more through study of the factors that enter into gravel pack design has been reported by Saucier (1974) including some hydrodynamic factors. He found that to minimize sand production without greatly increasing permeability the ratio of the pack media grain size to formation median grain size should be between 5 and 6 under disturbed flow conditions. Rounded pack grains result in lower pressure gradients and less packing variance than more angular particles.

II Remarkable cleaning properties of viscoelastic liquid films laden with small particles. Remediation of oil slicks.

This has to be seen to be believed. The withdrawal by suction of a particle-laden fluid of high concentration results in a complete removal of all fluid from the walls of the lower glass chamber. If there are no particles in the fluid, or the concentration of particles is less than 4%, a puddle of liquid is left behind. The full impact of this very unusual cleaning property requires the reader to view the movie sequences titled, "*Screening and cleaning properties*" which can be found on our web page, *http://www.aem.umn.edu/research/particles/siphon/*. The sequence is shown in Figure II.1.

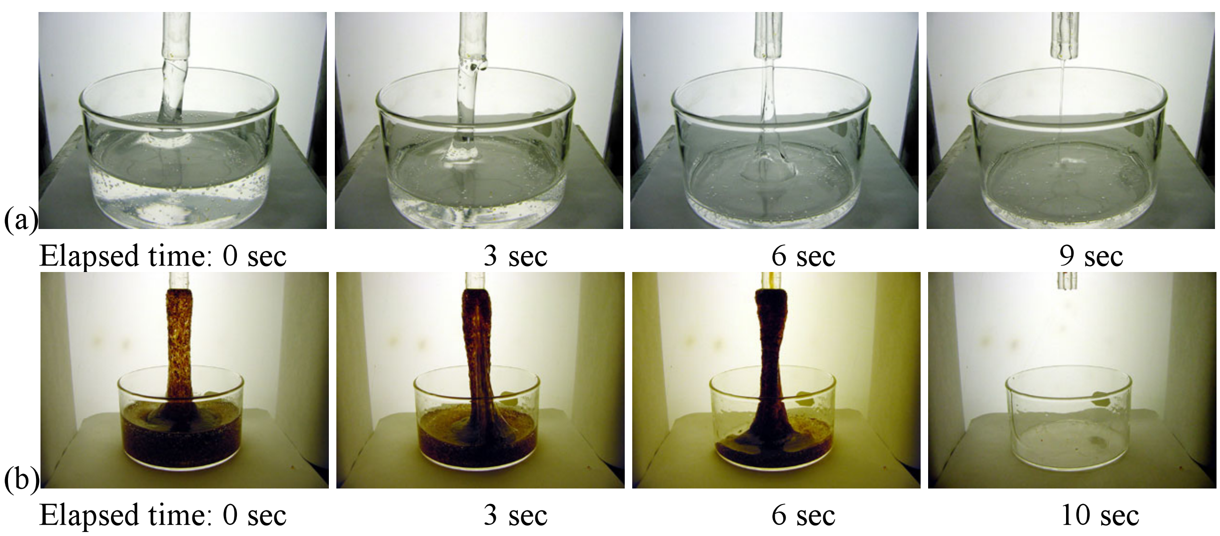

Figure II.1. Sequence of screening and cleaning properties of viscoelastic liquid films, (a) with a low concentration of particles (b) with a high concentration of particles. Click on the photograph sequence to view the movies.

The formation of the particle-laden fluid film is related to the screening property of particles which are lifted by the fluid and blocked from entering the tube (see figure I.2). The particles which are sucked up in the tubeless siphon appear to be trapped in the surface, with few or no particles inside. The cleaning properties of particle laden viscoelastic films might find good application in the removal of contaminants from a substrate.

The proposal projects are to evaluate the cleaning properties of films varying factors such as:

1. Type of viscoelastic fluids.
2. Size and concentration of particles.
3. Speed of withdrawal.
4. Properties of the substrate.

The cleaning properties of viscoelastic liquids are greatly enhanced by the presence of particles. However, we can clean the beaker in figure II.1 when there are no particles if the withdrawal rate is much higher. We need to generate very high extensional stress at high rates of pulling.

The experiments on cleaning of beakers suggest applications to remediation of oil slicks; if we can pull liquids off solid surfaces, maybe we can pull them off liquid surfaces. We did a preliminary experiment by spreading a slick of an oil based polymeric liquid on water. We drew off the slick (whose thickness is in nanometers) with a pipette and noted that at higher rates of sucking the slick moved strongly to the pipette from great distances as in figure I.5. We created an oil slick with motor oil. We could not draw oil and only water entered into the pipette. In contrast, when we spread the polymeric oil based liquid on top of the motor oil, a certain amount of mixing took place and we were able to suck off all the mixture.

Our working hypothesis is that if an oil slick is augmented with oil based polymeric liquid, the mixture can be drawn off from great distances by the long-range effects of extensional stresses that develop at high rates of sucking.

III Motions due to capillarity of floating particles on liquid surfaces

This aspect of our proposal is to study motions of floating particles in gas-liquid and liquid-liquid surfaces. Our goal is to characterize the motions of spherical and natural particles, sand, clay and other small particles especially in terms of size, weight, shape, concentration and wettability of particles.

The deformation of liquid-fluid interfaces due to floating light particles or due to trapped heavy small particles gives rise to capillary forces on the particles which cause them to cluster as in figure III.1. The qualitative nature of these forces can be explained by simplified arguments presented below.

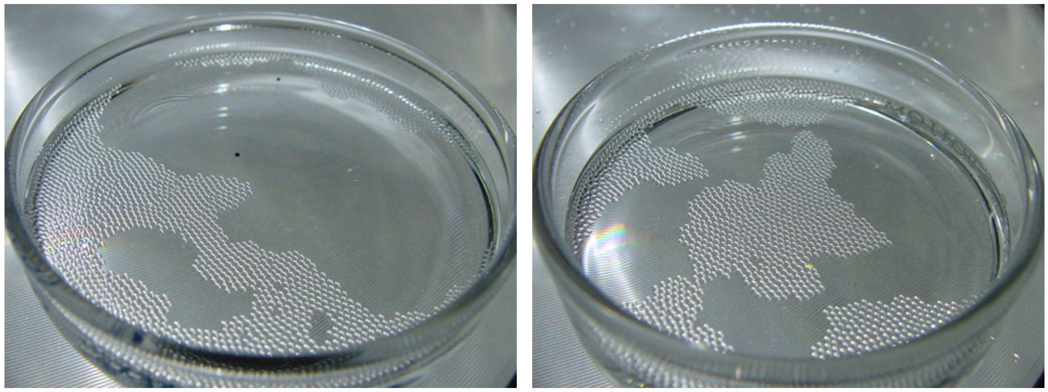

Figure III.1. Neutrally buoyant glass beads cluster in water.

III.1 Vertical force balances

The simplest analysis relevant to understanding the forces on small particles is the vertical force balance on a sphere floating on the interface between fluids which, for convenience, is here called water and air. This analysis was given first by Princen (1969), then by Rapacchietta and Neumann (1977) and more recently by Kotah, Fujita and Imazu (1992), who used the floating ball to measure contact angles.

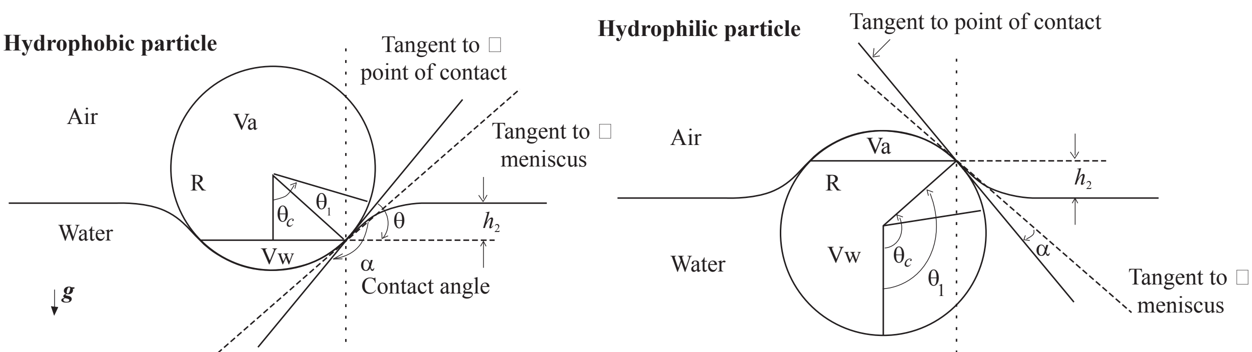

Figure III.1. Hydrophobic and hydrophilic particles in mechanical equilibrium. The position of the contact ring is determined θ_C. The point of extension of the flat meniscus on the sphere is given by θ_1.

The capillary force F_C, is a function of the radius of particle R, the surface tension coefficient γ, the filling angle θ_c and the contact angle α, given by,

$$F_C = 2\pi(R\sin\theta_c)\gamma\sin[\theta_c - (\pi-\alpha)] = -2\pi(R\sin\theta_c)\gamma\sin(\theta_c+\alpha) \qquad \text{(III.1)}$$

for both the hydrophobic case and the hydrophilic case.

From mechanical equilibrium, the capillary force must equal the vertical resultant of pressure around the sphere must balance the gravity vertical component:

$$F_C + F_p = G. \qquad \text{(III.2)}$$

where $\vec{e}_z$ is a unit vector opposing gravity (see figure I.2).

Use the pressure p_0 in the fluid at the height of the bottom of the sphere as the reference pressure. We have;

$$p(z) = p_0 - \rho_l gz = p_a + \rho_l g(h_1 - z) \quad \text{(III.3)}$$

With $\vec{e}_z \cdot \vec{e}_r = \cos(\pi - \theta) = -\cos\theta$ and $d\sum = 2\pi R \sin\theta \, R d\theta$ and z = R (1 - cosθ), (III.3) becomes:

$$\begin{aligned} F_p &= \int_\Sigma p \cdot 2\pi R^2 \sin\theta \cos\theta \, d\theta \\ &= \rho_l g\pi R^3 (\frac{2}{3} - \cos\theta_c + \frac{1}{3}\cos^3\theta_c) + \\ &\rho_a g\pi R^3 (\frac{2}{3} + \cos\theta_c - \frac{1}{3}\cos^3\theta_c) - (\rho_l - \rho_a) g h_2 \pi R^2 \sin^2\theta_c \end{aligned} \quad \text{(III.4)}$$

$V = \frac{4}{3}\pi R^3$ is the volume of the sphere; $v = \pi R^3 (\frac{2}{3} - \cos\theta_c + \frac{1}{3}\cos^3\theta_c)$ is the volume of the sphere immersed in the water and $A = \pi R^2 \sin^2\theta_c$ is the area of the ring of contact. Then we can rewrite (III.4) as:

$$F_p = \rho_l g v + \rho_a g(V - v) - (\rho_l - \rho_a) g h_2 A$$

The first two terms at the right hand side are in agreement with Archimedes' principle, while the term $(\rho_l - \rho_a) g h_2 A$ accounts for the meniscus effect. When a meniscus is present, the buoyancy calculated by Archimedes' principle $\rho_l g v + \rho_a g(V - v)$ not only lifts the sphere, but also the fluid in the meniscus. Hence, we need to subtract the weight of the lifted fluid from $\rho_l g v + \rho_a g(V - v)$ to get the buoyancy on the sphere. (III.4) implies that the volume of the lifted fluid is $h_2 A$.

Inserting (III.1) and (III.3) into (III.2), we get:

$$\begin{aligned} &\sin\theta_c \sin(\theta_c + \alpha) = -\frac{1}{2}\frac{\rho_l g R^2}{\gamma}[\frac{4}{3}\frac{\rho_p}{\rho_l} - (\frac{2}{3} - \cos\theta_c + \frac{1}{3}\cos^3\theta_c) - \\ &\frac{\rho_a}{\rho_l}(\frac{2}{3} + \cos\theta_c - \frac{1}{3}\cos^3\theta_c) + (1 - \frac{\rho_a}{\rho_l})\frac{h_2}{R}\sin^2\theta_c] \end{aligned} \quad \text{(III.5)}$$

Figure III.1 shows that $h_2 = R(\cos\theta_1 - \cos\theta_c)$, and equation (III.5) may be in dimensionless form

$$\begin{aligned} &\sin\theta_c \sin(\theta_c + \alpha) = -\frac{1}{2}B[\frac{4}{3}\psi_1 - (\frac{2}{3} - \cos\theta_c + \frac{1}{3}\cos^3\theta_c) - \\ &\psi_2(\frac{2}{3} + \cos\theta_c - \frac{1}{3}\cos^3\theta_c) + (1 - \psi_2)(\cos\theta_1 - \cos\theta_c)\sin^2\theta_c] \end{aligned} \quad \text{(III.6)}$$

where $B = \rho_l R^2 g/\gamma$ is the bond number and $\psi_1 = \rho_p/\rho_l$ and $\psi_2 = \rho_a/\rho_l$ are the dimensionless control parameters.

Several conclusions can be drawn from (III.5) or (III.6).

Small particles can be suspended in fluid surfaces no matter how heavy they may be provided

$$\frac{\rho_p R^2 g}{\gamma} \to 0 . \qquad \text{(III.7)}$$

Moreover, in this case sin (α + θ_C) = 0 and for hydrophobic particles

$$(\alpha + \theta_C) = 0 \left(\theta \le \alpha \le \frac{\pi}{2} \right) \qquad \text{(III.8)}$$

Of course, we could not measure α on a nanoparticle. Moreover, if the particle is irregular with sharp corners the capillarity argument fails. Liquid-air surfaces bind at razor sharp corners; the physics associated with this strong bond are not understood. Razor blades and straight pins can float on water-air surfaces pinned at the sharp surface.

Equations (III.7) and (III.8) suggest that hydrophobic nanoparticles can float on the surface no matter how heavy they are. However, even though the formula does not predict that hydrophilic particles will sink, they will sink because of a not-understood wetting instability.

Another conclusion, appropriate to large heavy particles, can be inferred from (III.5) or (III.6) following from the observation that the left side of these equations, consequently, the right sides, lie in the range $-1 \le \sin\theta_C \sin(\theta_C + \alpha) \le 1$. Obviously these equations cannot be solved if the particles are too large or too heavy.

III.2 Horizontal force balance

The deformation of a liquid-fluid interface due to trapped small particles gives rise to capillary forces exerted on the particle. These forces may be qualitatively understood from simple arguments. Two kinds of forces act on particles: forces due to gravity and forces due to the action of the contact angle. These two kinds of forces are at play in the vertical force balance but require a somewhat more elaborate explanation for the horizontal force balance. The effects of gravity are usually paramount for heavier-than-liquid floating particles in which one particle will fall into the depression of the second (see figure III.3). A heavier-than-liquid particle will fall down a downward sloping meniscus while an upwardly buoyant particle will rise.

There are several ways to isolate the effects of capillarity uninfluenced by gravity. Poynting and Thompson (1913) investigated the capillary effect by considering two vertical plates immersed in a liquid, the space between the plates is a two dimensional capillary tube. If the plates are hydrophobic, the level in the capillary gap sinks below the liquid outside; if the plates are hydrophilic the levels will rise. Their argument about the nature of horizontal forces on the plates is given in the caption of figure III.4. Repulsion between particles with different wetting properties is rather short range because it stops when the meniscus between particles gets flat.

Another way to take away the effects of gravity is to support the particles on a substrate. In this case the horizontal forces are due to capillary effects alone. Katoh *et al* wrote a paper on the "Motion of a Particle Floating on a Liquid Meniscus Surface[1]" which could be interpreted as motion on a substrate because the foaming phlystyrol particles used by them are an order of magnitude lighter than water, and minimize the effects of gravity compared to capillarity. Their

[1] Katoh, Fujita and Imazu (1992). *Journal of Fluids Engineering*, **114**, 411-416.

experimental results are completely consistent with the predictions of Poynting and Thompson[2]: when the sphere and the wall are alike with respect to wetting; say both are hydrophobic or hydrophilic, the wall and sphere attracts; when they are unlike the sphere and wall repel.

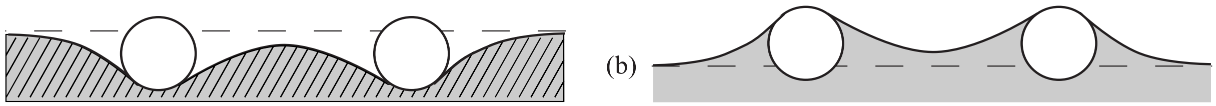

Figure III.3. Spherical particles in water, (a) heavier-than-water hydrophobic particles. The meniscus is below the undisturbed level. If the contact angle doesn't vary the particle must tilt causing an imbalance of the horizontal component of capillary forces pulling the spheres together. Even if the particles do not tilt they will both fall under gravity into the depression between them. (b) Heavier-than-air and lighter-than-water hydrophilic particles. The meniscus is above the undisturbed level. The particle must tilt giving rise to an imbalance of horizontal forces, drawing the particles together. Air bubbles come together.

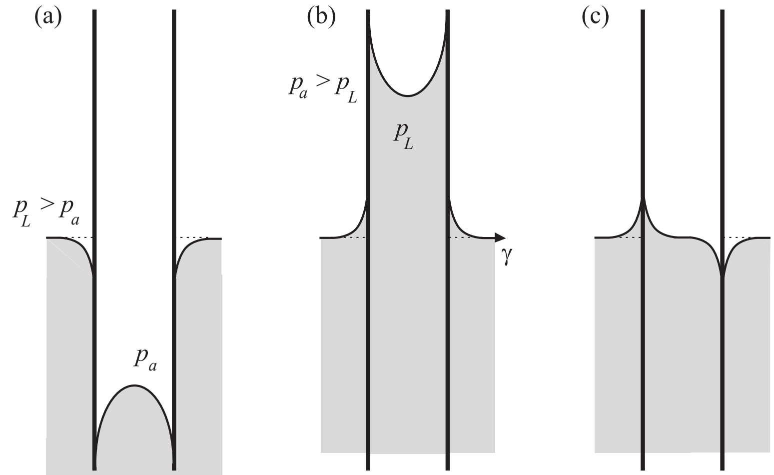

Figure III.4. (After Poynting and Thompson 1913). Horizontal forces associated with the fall (a) of liquid between hydrophobic plates and the rise (b) of liquid between hydrophilic plates. In (c) one plate is hydrophilic and the other hydrophobic. The contacts on both sides of a plate are the same and the tension γ is constant. They argue that the net horizontal force due to γ can be calculated at flat places; so that there is no net horizontal component of the tension. In (a) and (b) the pressures are such that they push the plates together; there is no net attractive force in (c). If the plates (c) are so close that there is no flat place, then the horizontal projection $\gamma \sin \alpha$ of the slope $\tan \alpha$ of the interface midway between the plates is smaller than the horizontal component γ outside the plates and the plate are pulled apart; they repel. They note that "… small bodies, such as straw or pieces of cork, floating on the surface of a liquid often attract each other in clusters; this occurs when the bodies are all wet by the liquid and also when none of them is wet; if one body is wet and one is not wet, they repel each other." (It may help here to note that if one face of the plate is hydrophobic and the other hydrophilic, the contact angles will put the plates in tension, tending to pull them apart.)

[2] The simple heuristic analysis of Poynting and Thompson is mentioned but not discussed by Nicolson (1949). Other authors seem not to have looked at this pioneering work even when, after extensive calculation, they reach exactly the same conclusions (see, for example, the conclusion of the paper by Fortes 1982).

Despite the well-established importance of the capillary meniscus forces there are only a few theoretical works devoted to them. Nicolson (1949) was the first to derive an analytical expression for the capillary force between two floating bubbles by using the superposition of approximation to solve the Laplace equation of capillarity. A similar approximate method was applied by Chan, Henry and White (1981) to floating spheres and horizontal cylinders. For horizontal cylinders the alternative approaches were proposed by Gifford and Scriven (1971) and by Fortes (1982). The theoretical works are based on solutions of the Laplace equations for capillary menisci of translational or rotational symmetry, where the Laplace equation reduces to an ordinary differential equation.

An analytical solution of the Laplace partial differential equation in bipolar coordinates was proposed by Kralchevsky, Paunov, Ivanov and Nagayama (1992) Kralchevsky, Paunov, Denkov, Ivanov and Nagayama (1993) for the case of small particles and small meniscus slope. This solution provides expressions for calculating the capillary meniscus force between two vertical cylinders, between two spheres partially immersed in a liquid layer and between a vertical cylinder and a sphere.

III.3 Dynamics

The dynamic behavior of fluid particles is not well understood. Gifford and Scriven (1971) note that "casual observations… show that floating needles and many other sorts of particles do indeed come together with astonishing acceleration. The unsteady flow fields that are generated challenge analysis by both experiment and theory. They will have to be understood before the common-place 'capillary attraction' can be more than a mere label, so far as dynamic processes are concerned."

The drag on a particle is important in describing its motion, and the dispersion (here anti-dispersion) could be modeled (but not well) by diffusion.

A small number of theoretical studies of the drag and diffusion coefficient of a spherical particle attached to a fluid interface (Brenner and Leal 1978, 1982; Goldman, Cox and Brenner 1967; Schneider, O'Neill and Brenner 1973; Majumdar, O'Neill and Brenner 1974—which may be collectively designated as Brenner *et al*—and Wakiya 1957; Redoev, Nedjalkov and Djakovich 1992; Danov, Aust, Durst and Lange 1995).

The only experimental determination of drag coefficients for particles of any size were determined by Petkov, Denkov, Danov, Velev, Aust and Durst (1995) for large particles of sub-millimeter radius by measuring the particle velocity under the action of well defined external force. They showed that the capillary interactions are quite strong and very long range. Accelerations, which are very great under many conditions of interest in this research, have not been studied before.

IV Studies of transient free motions leading to self-assembly of floating particles

We propose to study the transient free motion leading to self-assembly of floating particles and to symmetry breaking pattern formations under forced motions. Examples of free motions leading to self-assembly can be seen in the figures and animations to follow. We propose to use the tools of analysis following others and to implement two new approaches: direction numerical simulation (section V) and the method of correlations (section VI) to study these transient motions.

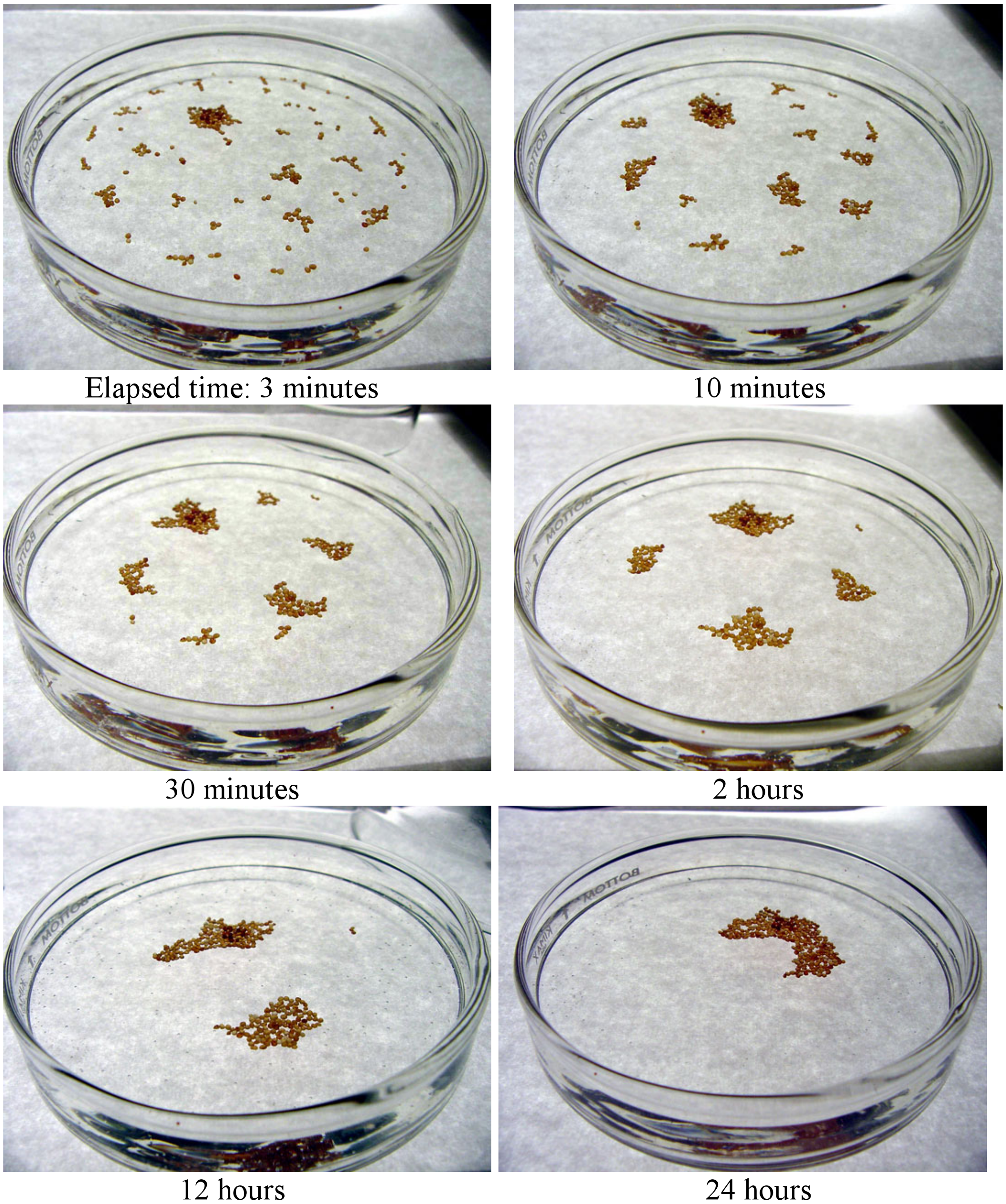

Figure IV.1. Free motions leading to self-assembly of floating particles. Click on the photograph "2 hours" to view a partial animation of the above sequence, which shows sands in 1% aqueous polyox solution. (http://www.aem.umn.edu /research/particles/sand_in_fluid/).

V Direct Simulation of Motion of Particles on Two-fluid Interfaces

In order to simulate the motion of rigid particles trapped on a two-fluid interface, we must solve the governing mass and momentum conservation equations for the two fluids, compute the forces acting on the particles and then move them according to the net force acting on them. This is clearly a difficult numerical task because the interface shape changes in response to the fluid motion and across the interface the fluid properties change suddenly and an interfacial force acts between the two fluids. In addition, we must prescribe the contact angle along the moving contact line on the particle surface. The contact line moves when the particle or the interface moves.

There are several numerical approaches available for tracking the interface between two immiscible liquids, e.g., the level set method (Osher and Sethian 1988, Sussman, Smereka and Osher 1994, Sussman and Smereka 1997, Sussman, Fatemi, Smereka and Osher 1998), the surface tracking method (Unverdi and Tryggvason 1992), the volume of fluid method (Fatemi and Odeh 1993, Hirt and Nichols 1981), the moving grid methods (Bousfield, Keunings and Denn 1988) and the mapping method (Ryskin and Leal 1984, Noh, Kang, and Leal 1993, Ramaswamy and Leal 1999a and 1999b). These methods have been used extensively to simulate viscous, inviscid and viscoelastic two-phase flows (Pillaipakkam and Singh 2001). In our work, we will use the level set method to track the interface. The level set method works efficiently on a regular fixed grid and thus is compatible with the distributed Lagrange multiplier method (DLM) which will be used to track the motion of rigid particles (Glowinski, Pan, Hesla and Joseph 1999, Singh, Joseph, Hesla, Glowinski and Pan 2000, Glowinski, Tallec, Ravachol and Tsikkinis 1992). The DLM method also works efficiently on regular fixed grids.

V.1 Numerical Method

To perform direct simulations, we must numerically integrate the mass and momentum equations for the fluid phases and the momentum equation for the rigid particles. The equations for the two fluid phases and the particles are coupled through the stress condition at the interface, and through the no-slip and hydrodynamic forces and torques which appear in the equation of motion for the rigid particles. In order to ensure stability when the time step is relatively large the partial differential equations must be solved simultaneously.

As we have noted above, in our finite element code the level-set method to track the interface position and the distributed Lagrange multiplier method is used to track the motion of rigid particles. The level set and DLM methods are compatible, as both perform efficiently on regular fixed grids.

The interface position in our code is tracked by using the level-set method (Osher and Sethian 1988, Sussman *et al* 1994, Sussman and Smereka 1997, Sussman *et al* 1998, Pillaipakkam and Singh 2001). In the level set method, the interface position is not explicitly tracked, but is defined to be the zero level set of a smooth scalar function ϕ, which is assumed to be the signed distance from the interface. In order to track the interface, the level set function is advected according the velocity field, i.e., $\frac{\partial \phi}{\partial t} + \mathbf{u}.\nabla\phi = 0$, where **u** is the fluid velocity. As ϕ is a smooth function, it is relatively easy to numerically solve the above equation to update the interface position. The method also allows us to enforce the contact angle on the rigid particle surfaces and it is relatively easy to implement it in both two and three dimensions.

The motion of particles is tracked using a distributed Lagrange multiplier method (DLM) (Glowinski *et al* 1999, Singh *et al* 2000, Glowinski, Tallec, Ravachol, Tsikkinis (1992). One of the key features of the DLM method is that the fluid-particle system is treated implicitly by using a combined weak formulation where the forces and moments between the particles and fluid cancel, as they are internal to the combined system. These internal hydrodynamic forces are not needed for determining the motion of particles. In our combined weak formulation we solve fluid flow equations everywhere in the domain, including inside the particles. The flow inside the particles is forced to be a rigid body motion using the distributed Lagrange multiplier method. This multiplier represents the additional body force per unit volume needed to maintain rigid-body motion inside the particle boundary, and is analogous to the pressure in incompressible fluid flow, whose gradient is the force needed to maintain the constraint of incompressibility.

As noted above, development of numerical schemes for simulating the motion of particles on the fluid interface is challenging because of the following problems in the governing equations of motion:

1. The domain is time-dependent in the sense that when the particles move the region occupied by the particles and fluids change.
2. The position of the interface evolves with time and the fluid properties change suddenly across the interface.
3. The incompressibility constraint and the nonlinear convection term which appear in the momentum equation.

In our numerical scheme the Marchuk-Yanenko operator splitting technique is used to decouple the difficulties associated with the incompressibility constraint, the nonlinear convection term, the rigid body motion constraint and the interface motion. The operator-splitting gives rise to the following four sub-problems: a Stokes-like problem for the velocity and the pressure; a nonlinear advection-diffusion problem for the velocity; a distributed Lagrange multiplier problem that forces rigid body motion within the particles; and an advection problem for the interface.

The decoupled sub-problems can be solved much more efficiently than the original problem (Glowinski *et al* 1999, Singh *et al* 2000, Glowinski *et al* 1992, Bristeau, Glowinski & Periaux 1987, Marchuk 1990, Singh and Leal 1993, Glowinski & O. Pironneau 1992). The first problem is solved by using a conjugate gradient (CG) method, and the second problem is solved by using a least-square conjugate gradient method (Glowinski *et al* 1992, Bristeau *et al* 1987). The third problem is for the distributed Lagrange multiplier that enforces rigid body motion inside the particles. This problem is solved by using a conjugate gradient method. The fourth problem is for the advection of interface which is solved using a third order upwinding scheme. The advected ϕ is then re-initialized to be a distance function using a novel fast algorithm developed by us (Pillaipakkam and Singh 2001). It is necessary to re-initialize ϕ to ensure that the scheme accurately conserves mass. In our code all of these sub-problems are solved using matrix-free algorithms which reduces the memory requirement of our code.

As discussed earlier, a particle trapped on a two-fluid interface is in a state of static equilibrium under the balance of buoyant weight and the capillary force which arises due to the deformation of the interface. In order to have equilibrium when the particle density is smaller than that of the lower liquid and larger than that of the upper fluid, the particle should be hydrophobic with respect to the lower fluid and hydrophilic with the upper fluid. The interface shape in this case is concave up and the net surface tension force acts against gravity. In this work we will assume that the dynamic contact angle is equal to the static contact angle.

Also notice that since the interface curvature around a suspended particle decreases with increasing distance from the particle, we may therefore define a region of influence for a suspended particle within which the interface deformation caused by it is not small. When a suspended particle is within the region of influence of another particle, it may move along the interface due to the sideways force that arises because of the surface deformation caused by the other particle (see figure V.1).

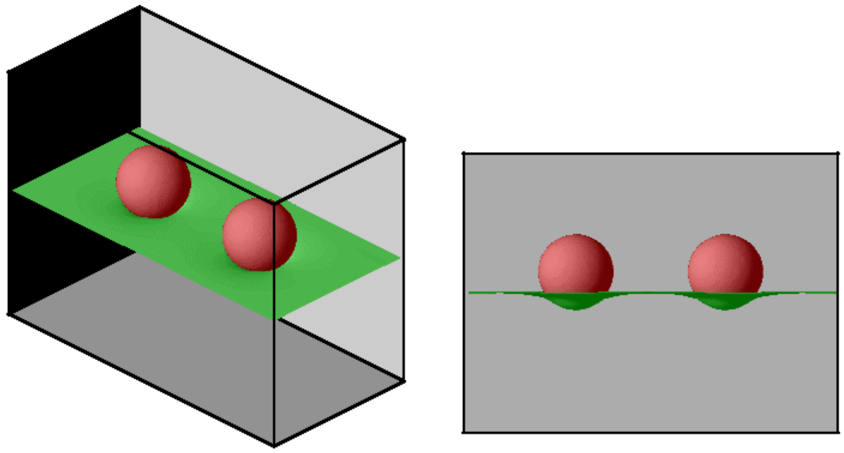

Figure V.1. The positions of two rigid particles suspended on the two-fluid interface are shown. They are moving towards each other on the interface. Notice that the particles are "supported" by the capillary force which arises due to the deformation of the interface. The surface tension is 70 dynes/cm, the particle density is 2.5 g/cm^3 and the density of the fluid on the top is 1.0 g/cm^3 and that on the bottom is 2.0 g/cm^3. The fluid viscosity is 1.0.

VI Method of correlations

The method of correlations is an old "tried and true" method of engineering analysis, which has been given a renewed impetus by the power of digital technology. To implement this data is it necessary to crate large data sets documenting some particular property. In the present case, we might consider the time to aggregation from some given initial condition, say of two particles or many particles. This is an experimental observable. The physical parameters believed to control this observable would then be listed on columns of a spread sheet; the viscosities, densities, wetting properties, interfacial tension are parameters to be listed together with parameter characterizing the initial conditions. The next step would be to attempt to identify dimensionless parameters controlling the observable; for example, the Bond number, density and viscosity ratios would enter as well as some presently unknown parameter associated with acceleration, viscous resistance and contact line resistance. Candidates for controlling dimensionless parameters, which is where the physics lie, could then be formed with a click of the mouse and plotted in log-log plots in a search for power laws. In our previous applications of this method to transport properties in solid-liquid and gas-liquid flows, power laws do emerge but the prefactors and exponents vary from system to system. Then in the same way the prefactor and exponents are processed for power laws. This also works in many cases. Identification of flow regime can also be done in these log-log plots where different power laws and transition regimes can be identified.[3]

The application of these methods to motions of particles in liquid surfaces has yet to be precisely formulated. The problem is very different and has features like interfacial forces at

[3] See *http://www.aem.umn.edu/research/particles/papers/* for a list of published papers that discuss this method. (Alternate site address: *http://www.aem.umn.edu/people/faculty/joseph/PL-correlations/* .)

sharp corners for which good theories do not exist. We think that we can shine a bright light on this field by generating and systematically processing data.

Other papers under review for publication are listed under the *Power law correlations* archive on the web site[3] just mentioned, and most are available for download.

VII Pattern formation arising in self-assembled aggregates of particles in fluid surfaces in forced motions.

In some sense this topic is the opposite to transient free motions leading to self-assembly; here the assemblies are dissembled into new patterns driven by forced motion. The motions of small particles on fluid surfaces can be viewed as dynamical systems. Concentrated aggregates of particles which are crystal-like when static will undergo symmetry breaking bifurcations when subjected to forced vibrations. Uniform dispersions of particles in a liquid film running the inside of a rotating cylinder can concentrate into bands of particles under the action of capillary force.

VII.1 Pattern formation arising from assemblies of particles under forced tangential motion

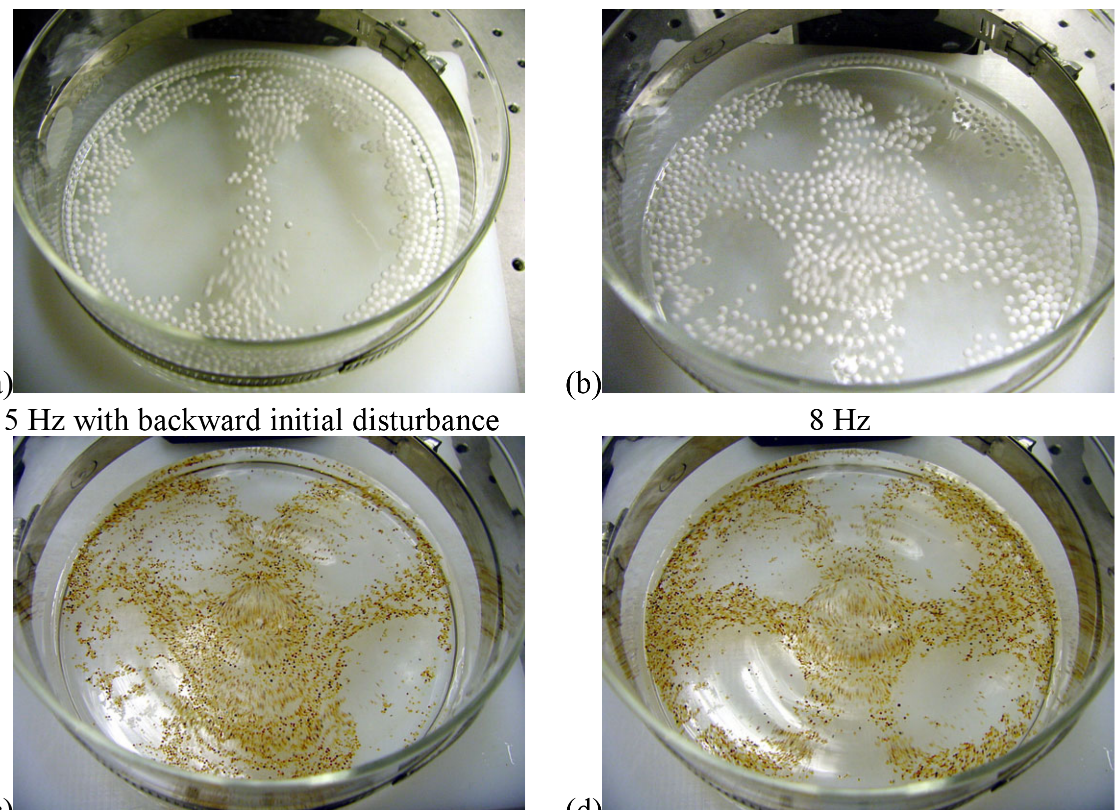

(a) 5 Hz with backward initial disturbance

(b) 8 Hz

(c) Elapsed time: 0 sec. at 8 Hz

(d) 12 sec. at 8 Hz

Figure VII.1. Pattern formation of particles under forced tangential motion. (a) (b) with light particles in water , and (c) (d) with slightly heavier-than-water particles. Click on the photograph(s) with a border to view its animation clip (or see http://www.aem.umn.edu/research/particles/shaker/).

VII.2 Particles segregation in a liquid film rimming a rotating cylinder

Tirumkudulu, Mileo and Acrivos (2000) (hereafter denoted as TMA 2000) observed that under certain circumstances particles which are initially distributed uniformly in a film rimming a horizontal rotating cylinder will be drawn into bands of high and low concentration. They did not offer a quantitative explanation of this phenomenon but suggested that the cause might be found in changes of the effective viscosity of the suspension induced by fluctuations of concentration.

Similar experiments were carried out at University of Minnesota. They identified two regimes in which particles segregate; a low-speed, low-Reynolds number regime, in which particles are segregated at thin places on the rimming film by capillary forces, and a high-speed regime associated with the development of hydrocysts (Balmer 1970, Karweit and Corrsin 1975, Preziosi and Joseph 1988 among others). The segregation at low Reynolds numbers occurs in the parameter ranges similar to those studied by TMA 2000. The high-speed segregation, which is not related to this proposal, has not been noted before.

- ***Particle segregation due to hydrocysts***

When an air-liquid mixture is spun rapidly in a rotating tube the phases will segregate due to centrifugal forces with heavy solids and liquids outside. The centrifugal forces suppress axial variation producing a long centrally located bubble with a uniform radius which may extend end to end if the speed of rotation is great enough. If the particles are heavier than the liquid, they will centrifuge into an axially uniform dispersion on the spinning wall. In principle, the cylindrical bubble will terminate at end caps produced by surface tension but it gets longer and longer as the rotational speed increases. The gas bubbles are no longer axisymmetric and they exhibit a dimple between liquid lenses separating the bubbles, where particles collect driven by secondary motion from the lens to dimple on the wall and dimple to lens near the bubble surface, as seen in figure VII.2.

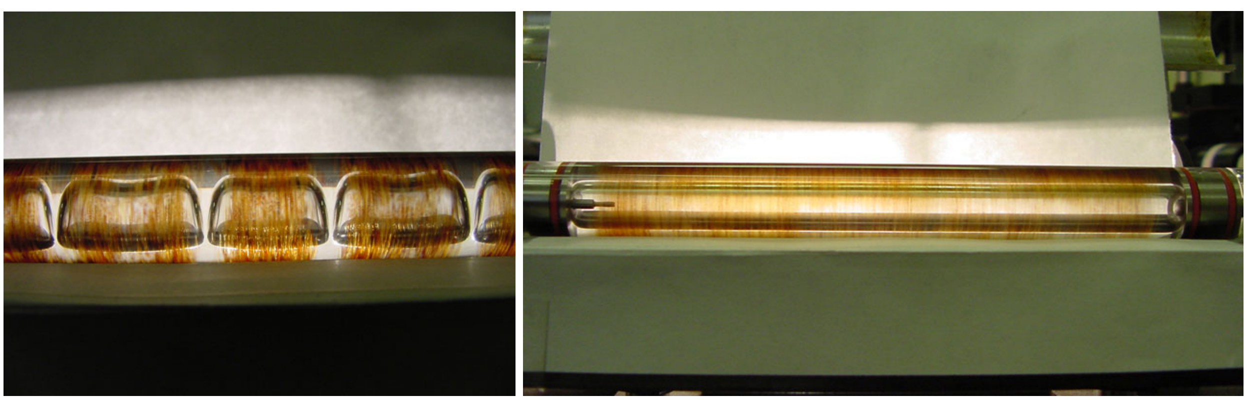

(a) (b)

Figure VII.2. Particle segregation due to hydrocysts. Air-soybean oil-particles (ρ_P = 1.05 g/cc, mean diameter d_m = 600 micron, concentration of the particles 15%, filling level 60%). (a) Ω = 600 rpm (b) Ω = 1000 rpm. Click on the photograph to view the movies on their web page (see http://www.aem.umn.edu/research/particles/hydrocysts/).

The formation of hydrocysts occur only under certain well-specified conditions (Preziosi and Joseph 1988.) They will not form in low viscosity fluids like water. The angular speed must be high enough to lift the bubble off the top wall but not so large that the liquid lenses between the bubbles break. The filling level must be rather large, of the order 50%. The particle segregation is driven by an axial gradient of centrifugal forces which is larger in the liquid lenses than at the dimple.

- ***Particle segregation due to capillarity***

This phenomenon occurs at very low Reynolds number and with small filling fractions. TMA 2000 found particle segregation in monodispersed sheared suspensions in a partially filled rotating horizontal cylinder when the filling fractures (liquid volume/total volume) were small $0.1 \leq F \leq 0.15$. The particle concentrations for the uniform mixtures were 5% and 15%. The appearance of segregated bands of particles was correlated with $\beta = F(gR/\Omega\nu)^{1/2}$ which is the only parameter that appears in lubrication theory for thin films. We have done experiments under similar, but not identical conditions, and in our case the segregation of particles is due to capillarity.

When a cylinder partially filled with a fluid mixture with small particles of the size used in the TMA 2000 experiment is turned a few times by hand and then put to rest so that a particle-laden fluid covers the whole cylinder, one can observe that particles trapped in the thin film at the top of the cylinder move rather rapidly together under the action of capillarity (see figure VII.3).

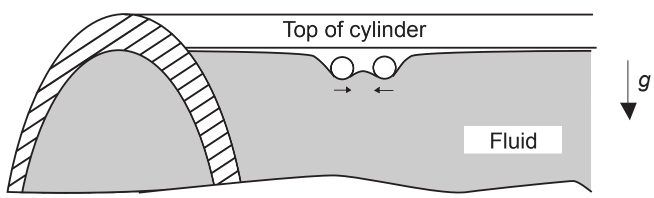

Figure VII.3. Capillary attraction of two particles hanging in a film at the top of a stationary rotating cylinder (cf figure VII.2).

A similar kind of dynamic prevails when the cylinder rotates continuously but very slowly as can be seen in figure VII.4; the collection of particles into bands takes hours to days, and the configurations which are achieved are stable only for times of the order of hours and days.

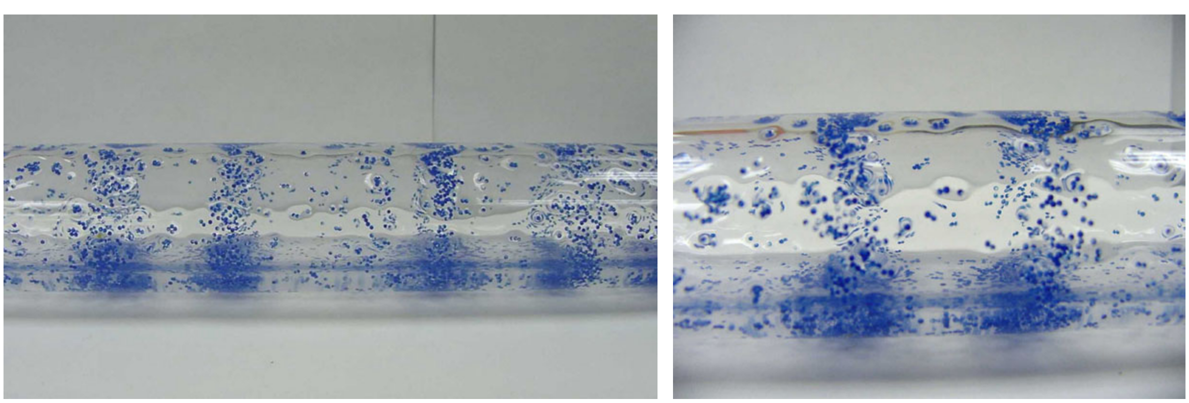

Figure VII. 4. Particles which are initially distributed uniformly in a film rimming a rotating cylinder will be drawn into bands. The fluid used here is a solution of $ZaCl_2$, Triton X100 and water. The rotating speed is 10.9 rpm and the formation of the bands takes hours. To view the animation click on each photograph or see http://www.aem.umn.edu/research/particles/rtcylinder/. The capillary attraction of neighboring particles can be clearly seen in the animation.

A comparison of the Minnesota experiments in figure VII.4 with one reported by TMA 2000 (their figure 2a) is given in table VII.1.

	F	R cm	μ poise	ρ om/cc	$\nu=\mu/\rho$	β	ρ_p gm/cc	d_p cm	Ω rpm
A	0.15	1.396	51.95	1.241	41.86	2.08	1.034	0.065	1.65
B	0.15	1.27	40	1.172	34.13	1.8	1.172	0.0462	1.4

Table VII.1. Comparison of (A) Minnesota experiment with (B) Tirumkudulu, Mileo and Acrivos (2000) or TMA. The particles used by TMA are more monodispersed than in those in figure VII.4. d_p *is the mean particle diameter.*

We have found particle segregation like that shown in figure VII.4 for other liquids and particles.

The goal of our research on particle segregation in a partially filled rotating cylinder is principally to establish the conditions under which particles segregate due to capillary attraction. In particular, we want to identify precisely the set of dimensionless parameters which control segregation due to capillarity. It is probable that an important parameter for this study is a ratio of the particle diameter to the minimum film thickness[4].

VIII Surface active properties of colloidal and nanoparticle embedded in liquid surfaces with application pointing to the stabilization of emulsions and core-annular flows.

Small particles are readily trapped in liquid-gas and liquid-liquid surfaces even when they are heavy (see equation (III.8) and the scanned photos and animations). Such particles are always surface active by virtue of the effects of capillarity and sometimes this activity mimics amphillic properties of surfactants. It is known since the pioneering works of Ramsden (1903), who observed that emulsions were stabilized by solid matter at the interface between liquids, and by Pickering (1907) who noted that colloid particles that were wetted more by water than by oil could act as an emulsifying agent for oil-in-water emulsions. Since then about ten or so papers have been written which are listed in papers by Menon and Wasan (1986) and by Yan and Masliyah (1994). It is generally accepted that *hydrophilic solids stabilize oil-water emulsions, while hydrophobic solids stabilize water-in-oil emulsions.*

By far the greatest interest has focused on stabilization of oil-water systems by colloidal clay particles; in fact these finely divided particles may be measured in nanometers. Manon and Wasan (1986) studied particle-fluid interactions in solids–stabilized emulsions using asphaltene-treated mineral particles. They found that the ability of the finely divided solids to stabilize the emulsions is due to the absorption of asphaltene which imparts hydrophobic characteristics to the mineral surface. They note that for clay particles "…hydrophobicity …arises from the absorption of asphaltines and resins from the oil onto the initially hydrophilic clay." The *degree* of hydrophobicity of clay particles in asphaltene-laden crudes is a mater of great interest to applications arising in oil technology in Canadian Tar sands and Orinico belt in Venezuela.

[4] Though TMA did not consider capillary attraction they did note that the particles did not return to the low concentration region because the minimum film thickness became comparable to the particle diameter, as is consistent with an explanation based on capillary attraction.

Self-Lubricated Transport of Heavy Crude Oil

"Powdering the dough"

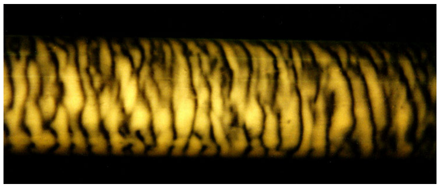

'Tiger' waves are on the black bitumen lubricated by released milky-white water with colloidal clay particles.

Scale-up for self-lubricated bitumen froth

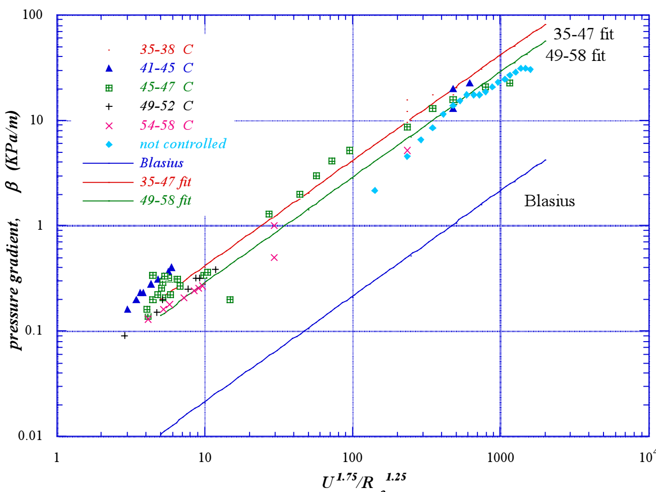

Phenomenon

- The phenomenon of self-lubrication was discovered while studying the effects of velocity and temperature on the flow of a mixture of heavy crude oil, sand and water (called *bitumen*) through a pipeline. The bitumen self-lubricates when flowing at speeds greater than critical where the mixture separates next to the pipe wall and lubricating films of clay water are formed. The clay protects the oil from sticking to itself and to the pipe wall—like flour "powdering the dough."

Achievements

- Models were developed to understand the critical conditions necessary for this phenomenon to occur at different pipe diameters. Using the reliability and scale-up results developed, a self-lubricated pipeline was built, 36 in. diameter and 35 km long, at a cost of $76M by a major oil company. This energy efficient line was put into operation in August 2000 and it transports bitumen at 3% of the cost without lubrication, a savings of 97%.

Figure VIII.1. "Bullet" description of self-lubricated pipelining of bitumen froth. This was selected by the Engineering Research Program of the Office of Basic Energy Sciences at the DOE as an example of exemplary energy research.

I am not aware of any industrial application of the stabilization of oil-in-water emulsions with clay particles. However, the "psuedo-amphillic" properties of such particles are essential for "self-lubricated" pipelines, which is described in the "bullet" in figure VIII.1 and in the paper by Joseph, Bai, Mata, Sury and Grant (1999). The last two authors named are from Syncrude, CA; the pipeline runs from the new Aurora mine to the upgrading facility at Lake Mildred.

Self-lubricated pipelines are low tech; basically if the bitumen froth, which is created by Clark's hot water extraction process, is put into a pipeline, and pumped fast enough, it will self-lubricate. This is due to the absorption of clay particles on the oil surface. In the hot extraction process for tar sands, the bitumen is leached from the surface of sand particles. Sand and clay particles present in the system form stabilizing films at the surfaces of bitumen-water emulsion droplets. The solid particles are attached to the bitumen on surfactant molecules, mainly asphaltines.

The "psuedo-amphilic" property seems not well understood. The clay particles do stick on the asphaltene, but they appear to retain their hydrophilic property on the walls in the water, and they do prevent the bitumen from sticking to itself. The fouled wall with clay covering is an excellent preparation for lubrication.

IX Nanoparticle assembly in vitrified liquid films

This is an idea we have not yet tried. We have not got resources for creating nanoparticles but we collaborate with colleagues (David Pui) that do have such resources. If an oily liquid is spread on water, it will form an oil slick. We may then load the film with hydrophobic heavier-than-water nanoparticles. The oil slick will coat the nanoparticles which may then become even more hydrophobic. The particles will self assemble under the action of capillarity. If the oil liquid can now be vitrified we would be able to remove or evaporate the water leaving behind a solid sheet of assembled nanoparticles.

References

Balmer, R.T. The hydrocyst—a stability phenomenon in continuum mechanics, *Nature* (London) **227**, 600 (1970).

Boonacker, N.T. *Filtration of particles suspended in Newtonian and non-Newtonian fluids*, Thesis, U of Minnesota (1999).

Bousfield, D.W., R. Keunings & M.M. Denn. Transient deformation of an inviscid inclusion in a viscoelastic extensional flow, *J. Non-Newtonian Fluid Mech.* **27,** 205 (1988).

Brenner, H. and L.G. Leal. *J. Colloid Interface Sci.* **65**, 191 (1978).

Brenner, H. and L.G. Leal. *J. Colloid Interface Sci.* **88**, 136 (1982).

Bristeau, M.O., R. Glowinski & J. Periaux. Numerical methods for Navier-Stokes equations. Application to the simulation of compressible and incompressible flows, *Computer Physics Reports,* **6**, 73 (1987).

Chan, D.Y.C., J.D. Henry Jr. and L.R. White. The interaction of colloidal particles collected at the fluid interface, *J. Colloid Interface Sci*. **79**, 410 (1981).

Coberly, C.J. and E.M. Wagner. Some considerations in the selection and installation of gravel packs for oil wells, *Pet. Tech*. Aug., 1-20 (1938).

Danov, K.D., R. Aust, F. Durst and U. Lange. Influence of the surface viscosity on the hydrodynamic resistance and surface diffusivity of a large Brownian particle, *J. Colloid and Interface Science*, **175**(1), Oct 36-45 (1995).

Fatemi, E., F. Odeh. Upwind finite difference solution of Boltzmann equation applied to electron transport in semiconductor devices, *J. Comput. Phys.* **108**, 209 (1993).

Fortes, M.A. Attraction and repulsion of floating particles, *Can. J. Chem.* **60,** 2889 (1982).

Gifford, W.A. and L.E. Scriven. On the attraction of floating particles, *Chem. Engrg. Sci.* **26**, 287-297 (1971).

Glowinski, R., T.W. Pan, T.I. Hesla & D.D. Joseph. A distributed Lagrange multiplier/fictitious domain method for particulate flows, *Int. J. Multiphase Flows* **25(5)**, 755 (1999).

Glowinski, R. and O. Pironneau. Finite element methods for Navier-Stokes equations, *Annu. Rev. Fluid Mech*. **24**, 167 (1992).

Glowinski, R., P. Tallec, M. Ravachol & V. Tsikkinis. Chap. 7 in *Finite Elements in Fluids, Vol 8*, Ed. T.J. Chung, Hemisphere Publishing Corp., Washington DC (1992).

Goldman, A.J., R.G. Cox and H. Brenner. *Chem. Eng. Sci*. **22**, 637-653 (1967).

Hill, K.E. Factors affecting the use of gravel in oil wells, *Oil Weekly,* May 26, 13-20 (1941).

Hirt, C.W. and B.D. Nichols, Volume of fluid (VOF) methods for the dynamics of free boundaries, *J. Comput. Phys.* **39**, 201 (1981).
Joseph, D.D., R. Bai, C. Mata, K. Sury and C. Grant. Self-lubricated transport of bitumen froth, *J. Fluid Mech.* **386**, 127-148 (1999).
Karweit, M.J. and S. Corsin. Observation of cellular patterns in a partly filled, horizontal, rotating cylinder, *Phys. Fluids* **18**, 111 (1975).
Katoh, K., H. Fujita and E. Imazu. Motion of a particle floating on a liquid meniscus surface, *J. Fluids Engrg.* **114**, 411 (1992).
Kralchevsky, P.A., V.N. Paunov, N.D. Denkov, I.B. Ivanov and K. Nagayama. Energetical and force approaches to the capillary interactions between particles attached to a liquid-fluid interface, *J. Colloid and Interface Sci.* **155**, 420-437 (1993).
Kralchevsky, P.A., V.N. Paunov, I.B. Ivanov and K. Nagayama. Capillary meniscus interactions between colloidal particles attached to a liquid-fluid interface, *J. Colloid Interface Sci.* **151**, 79 – 94 (1992).
Manon, V.B. and D.T. Wasan. Particle-fluid interactions with application to solid-stabilized emulsions. Part 1, The effect of asphaltene adsorption. *Colloids Surf.* **19**, 89-105 (1986).
Majumdar, S.R., M.E. O'Neill, and H. Brenner. *Mathematika,* **21**, 147 (1974).
Marchuk, G.I. Splitting and alternate direction methods. *Handbook of Numerical Analysis*, P.G. Ciarlet and J.L. Lions (Eds.), Volume I, 197-462. Amsterdam: North-Holland (1990).
Nicolson, M.M. The interaction between floating particles, *Proc. Cambridge Philosophical Soc.,* **45**, 288 (1949).
Noh, D.S., I.S. Kang, & L.G. Leal. Numerical solutions for the deformation of a bubble rising in a dilute polymeric fluids, *Phys. Fluids,* **5(6),** 1315 (1993).
Osher, S. and J.A. Sethian. Fronts propagating with curvature-dependent speed: Algorithms based on Hamilton-Jacobi formulations, *J. Comput. Phys.* **83**, 12 (1988).
Petkov, J.T., N.D Denkov, K.D Danov, O.D. Velev, R. Aust and F Durst. Measurement of the drag coefficient of spherical particles attached to fluid interfaces, *J. Colloid and Interface Science,* **172**, 147-154 (1995).
Pickering, S.U. *J. Chem. Soc.* **91**, (1907).
Pillaipakkam, S.B. and P. Singh. A Level Set Method for computing solutions to viscoelastic two-phase flow, *J. Computational Physics,* **174**, 552-578 (2001).
Poynting, J.H. and J.J. Thompson. *A Text-book of Physics: Vol. 1, Properties of Matter*, C. Griffith & Co. Ltd (London) 153-155 (1913).
Preziosi, L., D.D. Joseph, 1988. The run-off condition for coating and rimming flows, *J. Fluid Mech.*, **187**, 99-113.
Princen, H.M. *Surface and Colloid Science*, E. Matijevie, ed., Interscience, New York, Vol. 2, p.1 (1969).
Ramaswamy, S. & L.G. Leal. The deformation of a viscoelastic drop subjected to steady uniaxial extensional flow of a Newtonian fluid, *J. Non-Newtonian Fluid Mech.* **85**, 127 (1999a).
Ramaswamy, S. & L.G. Leal. The deformation of a Newtonian drop in the uniaxial extensional flow of a viscoelastic liquid, *J. Non-Newtonian Fluid Mech.* **88,** 149 (1999b).
Ramsden, W. *Proc. Roy. Soc. London.* **72**, 156 (1903).
Rapacchietta A.V. and A.W. Neumann. Force and free-energy analyses of small particles at fluid interfaces: II. Spheres, *J. Colloid and Interface Sci.*, **59**(3), 555-567 (1977).
Redoev, B., M. Nedjalkov and V. Djakovich. *Langmuir,* **8**, 2962 (1992).
Ryskin, G. & L.G. Leal. Numerical solution of free-boundary problems in fluid mechanics. Part 1: The finite-difference technique, *J. Fluid Mech.* **148**, 1 (1984).

Saucier, R.J. Consideration in gravel pack design, *J. Pet. Tech*. Feb., 205-212 (1974).
Schneider, Y.C., M.E. O'Neill, and H. Brenner. *Mathematika,* **20**, 175 (1973).
Singh, P. & L.G. Leal. Finite element simulation of the start-up problem for a viscoelastic fluid in an eccentric rotating cylinder geometry using a third-order accurate upwind scheme, *Theor. Comput. Fluid Mech.* **5,** 107 (1993).
Singh, P., D.D. Joseph, T.I. Hesla, R. Glowinski & T.W. Pan. A distributed Lagrange multiplier/fictitious domain method for viscoelastic particulate flows, *J. Non-Newtonian Fluid Mech.* **91**, 165 (2000).
Sussman, M., E. Fatemi, P. Smereka & S. Osher. An improved level set method for incompressible two-phase flows, *Computers & Fluids,* **27**, 663 (1998).
Sussman, M. & P. Smereka. Axisymmetric free boundary problems, *J. Fluid Mech*. **341**, 269 (1997).
Sussman, M., P. Smereka & S. Osher. A level set approach for computing solutions to incompressible two-phase flow, *J. Comput. Phys.* **114**, 146 (1994).
Tirumkudulu, M., A. Mileo, A. Acrivos. Particle segregation in monodisperse sheared suspensions in a partially filled rotating horizontal cylinder, *Phy. Fluids*, **12**(6), 1615 (2000).
Unverdi, S.O. & G. Tryggvason. A front-tracking method for viscous, incompressible, multi-fluid flows, *J. Comput. Phys.* **100**, 25 (1992).
Wakiya, S. *Colloid Eng. Res. Rep*. **6**, March 30 (1957).
Winterburn, R. Control of unconsolidated sands in Wilmington Oil Field, *Drill. and Prod. Prac.* API 63-79 (1947).